

# Multiple Watermark Scheme based on DWT-DCT Quantization for Medical Images

Jianfeng Lu<sup>a</sup>, Meng Wang<sup>a</sup>, Junping Dai<sup>b</sup>, Qianru Huang<sup>a</sup>, Li Li<sup>a,\*</sup> and Chin-Chen Chang<sup>c,d,\*</sup>

<sup>a</sup>Institute of Graphics and Image  
Hangzhou Dianzi University  
Zhejiang 310018, China

jflu@hdu.edu.cn; 422326989@qq.com; lili2008@hdu.edu.cn

<sup>b</sup>Institute of Digital Media  
Hangzhou Dianzi University  
Zhejiang 310018, China  
djp@hdu.edu.cn

<sup>c</sup>Department of Information Engineering and Computer Science  
Feng Chia University  
Taichung, 40724, Taiwan

<sup>d</sup>Department of Information Engineering and Computer Science  
Asia University  
Taichung, 41354, Taiwan  
alan3c@gmail.com

Received July, 2014; revised February, 2015

---

**ABSTRACT.** In this paper, a multiple watermark scheme for medical images is proposed. The image feature information and private tag information are embedded into the original image as watermarks. Firstly, the medical image is divided into the region of interest (ROI) and region of non-interest (RONI). Secondly, a 2-level discrete wavelet transform (DWT) is applied in the ROI. The watermark is embedded using the low-frequency subband (LL2) of the DWT through quantizing the low-frequency coefficients. Finally, the RONI is divided into non-overlapping  $8 \times 8$  blocks. A discrete cosine transform (DCT) is used for each block, and the DCT coefficients of each block are sorted using zigzag transform. Seven intermediate frequency coefficients are selected to embed watermark by quantizing them. Then the feature information is embedded in the ROI and is semi-fragile, whereas the tag information is embedded in the RONI. The experimental results showed that our scheme has the advantages of lower error rate, strong robustness and high capacity for the watermarking algorithm applied in the RONI. Performance evaluation is made by calculating PSNR and SSIM to verify the accuracy of the algorithm.

**Keywords:** Medical image, Multiple watermark, Quantizing, ROI, RONI, DWT, DCT, Zigzag

---

**1. Introduction.** With the development of the Internet and the advent of Picture Archiving and Communication Systems(PACS), digital medical images can be transmitted expediently and quickly. In recent years, doctors have been able to transmit images to hospitals all over the world to seek high quality diagnoses or other diagnostic opinions [10]. When vast quantities of medical images are transmitted over the Internet, the content of an image can easily be attacked or tampered with, either incidentally or maliciously. The digital watermark that contains the patients name, gender, and birthday, along with the institution name, date of the last calibration, and other important information is embedded in a medical image to maintain the consistency of the diagnostic data and prevent

data tampering and forging. In addition, private data elements can be added to the medical image dataset as their own particular watermarks in order to track the image users. The image itself has features that include color, texture, shape, and spatial relationship features. These features can provide tracking information when the image changes. Thus, the feature information can be hidden in a medical image in the form of a watermark.

In recent years, many watermarking algorithms for medical images have been developed. Dong et al. [5] proposed a watermarking algorithm for medical images that used a part of a sign sequence as an unchangeable feature vector before the watermark was embedded into the image and after the watermark was extracted from the image. This sign sequence is obtained by distinguishing the symbols of DCT coefficients. A watermark is encrypted using a logistic map to enhance its confidentiality. Although the encryption and zero-watermarking technology are applied in the algorithm, it cannot resist most geometric attacks. Feng et al. [7] presented a fragile watermarking scheme based on IWT in order to carry out fast and robust certification for medical images. First, the algorithm uses quad-trees structures obtained by wavelet decomposition to embed watermarks. A combination consisting of the statistical information on the nodes of the quad-trees and the secret key is chosen to embed the watermarks. Then, one bit of the watermark is embedded into the chosen locations. However, this watermark is fragile. If the image-embedded watermark is non-maliciously attacked, the watermark will be completely destroyed, which will prevent the watermark information from being extracted. Gu et al. [10] presented a reversible watermark scheme for medical images. They divided a cover image into non-overlapping blocks and IWT is used in each block. Next, the energy of each block is determined, and the blocks are divided into three categories based on these energies. Finally, a histogram shifting method is used to embed watermarks with different sizes. Zhang et al. [29] proposed a semi-fragile watermarking scheme to improve the speed of the watermark embedding process. The algorithm divides the image into 4 × 4 blocks and applies a one-level integer wavelet transform to each block. The maximum low-frequency coefficient is adjusted in order to avoid checking the overflow of the pixel gray value. The algorithm is sensitive to malicious tampering and can resist image compression. However, it has false alarm pixels without applying a cumulative weighted voting method for a binary error map.

In this paper, a novel watermarking algorithm is proposed based on the use of multiple watermarks for Computed Tomography(CT) images. The entire medical image is divided into ROI and RONI. The image feature information is embedded in the ROI, and the private tag information is embedded in the RONI. The watermark in the ROI is used to detect image tampering, and the watermark in the RONI is robust to several signal processing techniques. Therefore, this method is suitable for most medical images.

## 2. Methodologies.

**2.1. DWT.** By applying L-level DWT [24] to the ROI, we get the low-frequency sub-band and high-frequency sub-band of the image, which correspond to the approximate component and detail component respectively. By embedding the watermark information in the low-frequency sub-band, the image can have better imperceptibility, and the watermark can also have a higher robustness. Changing the low-frequency sub-band coefficients may cause pixel changes in the relative positions of the spatial domain. This characteristic of the DWT can be used to detect tampering in medical images.

**2.2. Logistic System.** Because the digital watermarking information in a medical image is the feature information extracted from the original image, the watermark can be extracted in public. Maliciously tampering with the image will cause serious problems.

Thus, the digital watermark information should be encrypted before being embedded in the medical image.

A logistic map is a very simple type of chaotic mapping. It has been widely used in the field of security and communication. Its mathematical expression can be shown as follow [15].

$$X_{n+1} = \mu X_n(1 - X_n), \mu \in [0, 4], X \in [0, 1], \quad (1)$$

in the formula,  $\mu$  is parameter of the logistic map. Research revealed that a logistic map is in a chaotic state when  $X \in [0, 1]$ . In other words, the sequence produced by a logistic map is non-periodic and non-convergent with an initial condition  $X_0$ . When  $3.5699456 < \mu \leq 4$ , the value of  $\mu$  is especially close to 4. The value of the sequence generated iteratively presents a pseudo-random distribution state.

**2.3. Arnold Transform.** A two-dimensional Arnold transform is shown as follow [27].

$$\begin{pmatrix} x' \\ y' \end{pmatrix} = \begin{pmatrix} 1 & 1 \\ 1 & 2 \end{pmatrix} \begin{pmatrix} x \\ y \end{pmatrix} \bmod H \quad (2)$$

where  $x$  and  $y$  are the coordinates of the pixel,  $H$  is the height or width of the square image that is processed, and  $x'$  and  $y'$  are the coordinates of the scrambled image. The transform changes the position of two pixels, and if it is applied several times, a disordered image can be generated. The cycle of the Arnold transform will be calculated as the key when the watermark is decrypted.

### 3. The Proposed Scheme.

**3.1. Image Segmentation Of ROI.** Thresholding is one of the most powerful techniques for image segmentation. In our scheme, the OTSU algorithm is used to generate the threshold value for medical image binarization. Detecting the connected region can ensure the bounding box of the main organ area called ROI. The size and position of the ROI are transmitted as a key. The size of the ROI is extended to the multiple of 4 because the DWT level is 2 in this paper. Figure 1 shows the generating process of ROI in medical images.

**3.2. Image Segmentation Of RONI.** We have determined the position of the ROI in the medical image. After the ROI is cropped, select a region from the rest regions as RONI and the size of RONI based on the capacity of watermark. The position and size of the RONI are tested until its boundary can be divided by 8 because the block size of RONI is  $8 \times 8$ . So we can segment the RONI by cropping from the region after cropping ROI.

### 3.3. Feature Extraction From Medical Image.

**Step 1. Generating watermark containing region feature information.** Medical images primarily show human organs. These organs such as the lungs or brain always have fixed shapes. The area, area ratio, solidity, eccentricity, and perimeter of the ROI are extracted as watermark information from binary image of the ROI. The watermark is embedded into ROI. If someone tampers with the content of ROI maliciously, the binary watermark error map can locate the tampering position. Area of the region is obtained by counting the number of pixels on the connected region. Area ratio is obtained by dividing the value of this area by the size of the ROI. It reflects the degree of the connected regions extended range. The solidity is calculated by dividing the value of the area by the total number of white pixels on the minimum convex polygon. And it reflects the degree of the connected regions solidity. The eccentricity can be obtained by counting the ratio

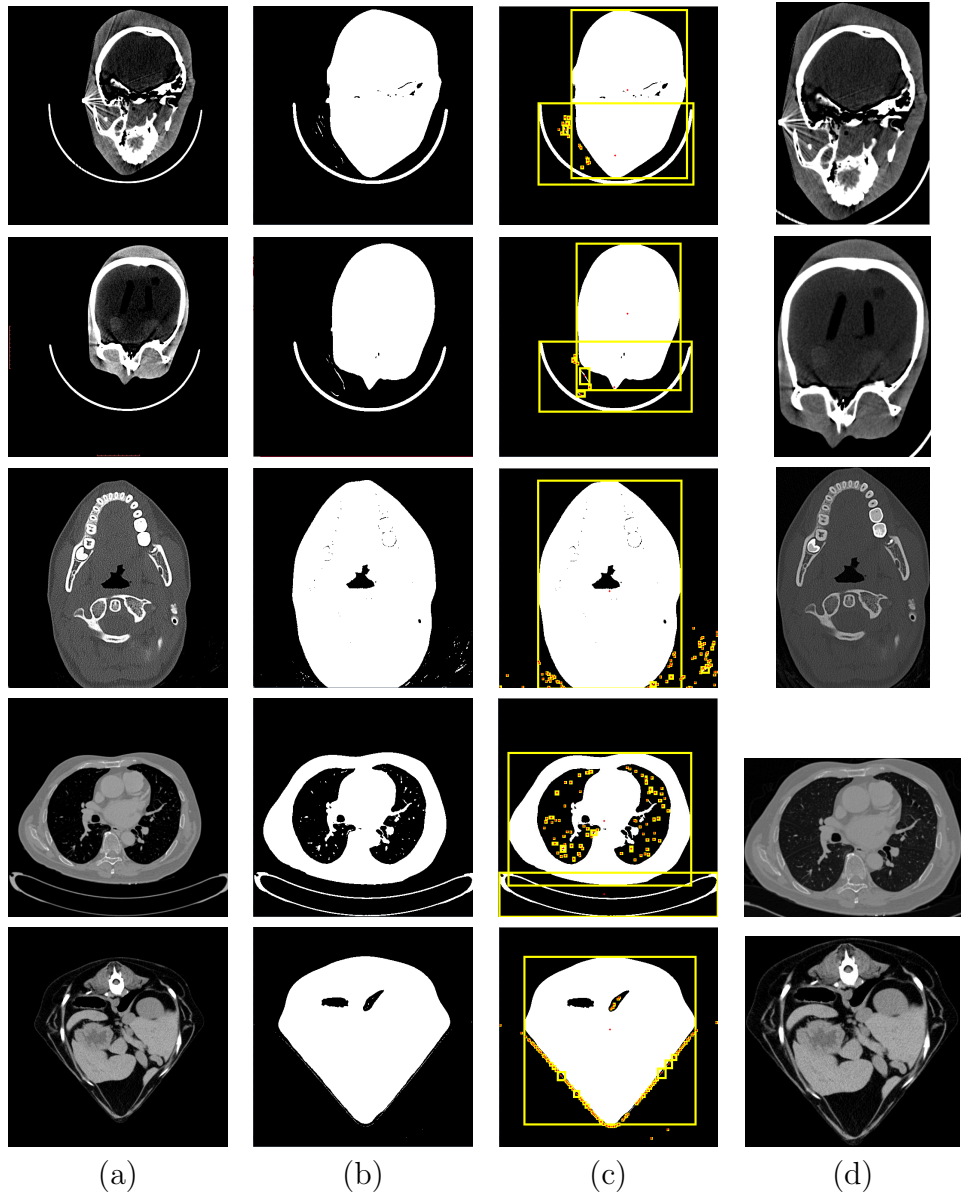


FIGURE 1. (a) Original medical images; (b) Medical image binarizations; (c) Bounding box of the connected region in medical images; (d) ROI cropped from (a)

of the focal length and major axis of the ellipse. The perimeter is obtained by counting the eight external chain code of the connected region. Figure 2 shows the watermark generated from the ROI.

**Step 2. Generating watermark containing tag information.** A medical image can be decoded according to the DICOM standard. The data set in the image is composed of a series of data elements. Each data element has a tag with only 4 bytes, where the first 2 bytes of the tag contain the group number of data elements. The data elements contain information related to the medical image. The patients institution name, gender, and birthday, along with the date of the last calibration are selected as the watermarking information. The odd group numbers are private data elements, and users can define these data elements themselves. When a user downloads the medical image on the network, the users account information will simultaneously be embedded into the private tag of the

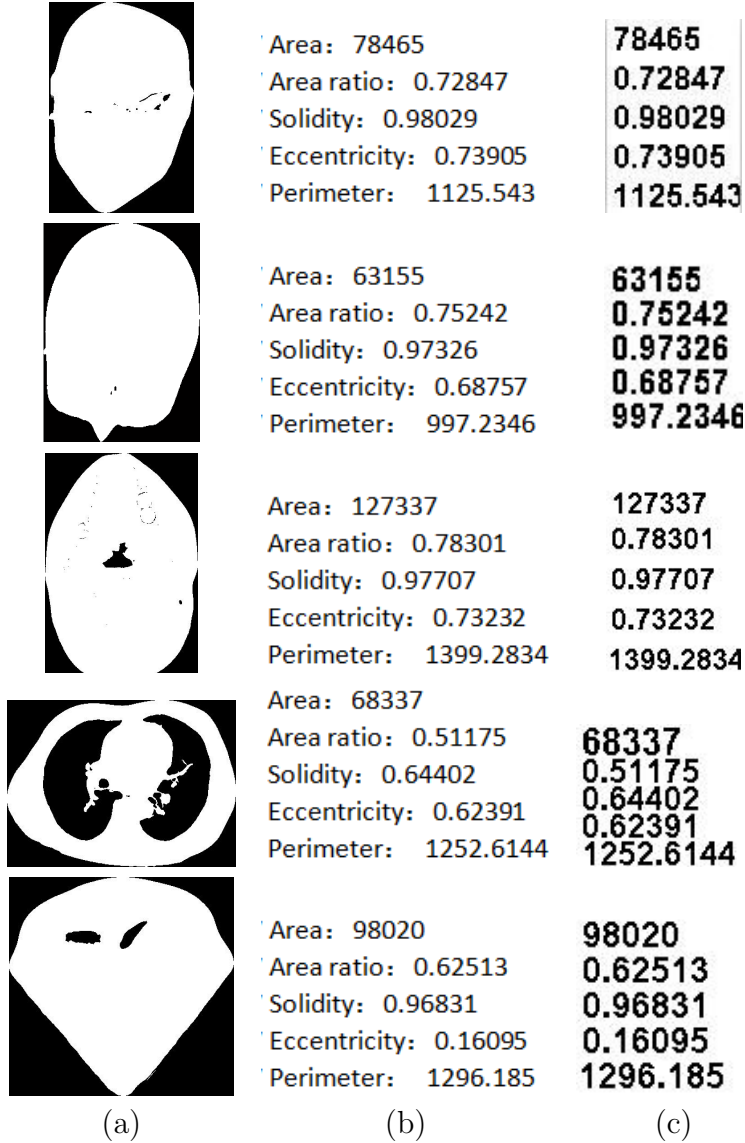


FIGURE 2. (a) ROI binarizations; (b) Feature information of ROI; (c) Watermark binarizations

medical image. The secret information in the binary image is embedded into the RONI as the watermarking information.

### 3.4. Embedding Scheme.

### Step 1. Watermark Embedding for ROI.

1) First, we decompose the ROI into two levels using DWT to get a low-frequency component and six high-frequency components. The low-frequency component is important. Its size is 1/4 of the ROI. The watermark will be embedded into these significant coefficients.

2) The quantization step is calculated according to the watermark embedding strength, the value of quantization step is inversely proportional to image distortion. Therefore, the watermark embedding strength in these complex textural regions is strong, and the watermark embedding strength in the smooth regions is weak. In the complex textural regions, the value of low-frequency coefficients and the value of high-frequency coefficients at the same decomposition level are large. In addition, the value of the quantization step calculated according to the formula is large. Thus, the watermark embedding strength

is adaptive to the regional characteristics. The calculation formula for the quantization step is shown as follow.

$$Q = k \cdot \ln \frac{|LH_2| + |HL_2| + |HH_2|}{2} \quad (3)$$

where  $k$  presents the quantization step coefficient;  $LH_2$ ,  $HL_2$ , and  $HH_2$  are high frequencies after the two-level wavelet decomposition.

3) The low-frequency coefficients are quantified by the quantization step. The formula is shown as follow.

$$X_Q = \lfloor LL_2/Q \rfloor \quad (4)$$

where  $LL_2$  is the low-frequency component that is chosen to embed the watermark.

4) The watermarking image is encrypted using the logistic map. When  $X_1 = 0.9$  and  $\mu = 3.95$ , a pseudo-random sequence is generated though the logistic system, and a binary sequence is obtained though these values, which have been rounded off. The one-dimensional binary sequence is extended to the two-dimensional binary matrix  $S$ , which has the same size as the watermarking image.

$$S = \{s(i, j) \in \{0, 1\}, i = 1, 2 \dots M/2^L, j = 1, 2 \dots N/2^L\} \quad (5)$$

where  $M$  is the width of  $S$ , and  $N$  is the height of  $S$ . The encrypted watermarking image  $W_{sROI}$  is obtained by applying an  $XOR$  operation to the original watermarking image  $W_{ROI}$  and the two-dimensional matrix  $S$ .

$$W_{sROI} = W_{ROI} \bigoplus S \quad (6)$$

5) The low-frequency coefficients are modified using the following formula.

$$LL'_2 = \begin{cases} X_Q \cdot Q & \text{if } mod(X_Q, 2) = W_{(i)sROI} \\ X_Q \cdot Q + Q & \text{if } mod(X_Q, 2) \neq W_{(i)sROI} \end{cases} \quad (7)$$

where  $LL'_2$  is low-frequency component after modification.

6) After embedding all of the watermarking, the low-frequency coefficients and other unmodified high-frequency coefficients are combined. Then, the inverse DWT is applied for reconstructing and creating the watermarked ROI.

## Step 2. Watermark Embedding for RONI.

1) The RONI is divided into non-overlapping  $8 \times 8$  blocks. Then, the DCT transform is applied to each block.

2) The coefficients of each block are sorted using a zigzag sequence and get a one-dimensional row vector. The zigzag sequence is marked off with numbers as Table 1.

TABLE 1. The zigzag sort

1	2	6	7	15	16	28	29
3	5	8	14	17	27	30	43
4	9	13	18	26	31	42	44
10	12	19	25	32	41	45	54
11	20	24	33	40	46	53	55
21	23	34	39	47	52	56	61
22	35	38	48	51	57	60	62
36	37	49	50	58	59	63	64

3) If the watermark is embedded in the low-frequency components, it will cause image distortion. If the watermark is embedded in the high-frequency components, the watermarking information will be lost if the image is filtered and quantified. Embedding the watermark in the middle-frequency coefficients is an eclectic method. Therefore, the frequency coefficients from 13 to 19 are selected to embed the watermarking information.

4) The quantization formula used to quantify all the middle-frequency coefficients from each  $8 \times 8$  block is shown as follow.

$$Z_q = \text{round}(I_{dct}/q) \quad (8)$$

where  $Z_q$  is the middle-frequency vector after quantifying.  $I_{dct}$  is the original middle-frequency vector, and  $q$  is the quantification step.

5) The original watermarking image is scrambled using the Arnold transform, and the image is unrecognizable. Then, we get the encrypted watermark image  $W_{nRONI}$ . The iteration number is  $n = 10$ .

6) For all the  $8 \times 8$  blocks, the watermark embedding formula is shown as follow.

$$I'_{dct} = \begin{cases} (Z_q - 1/2) * q, & \text{if } \text{mod}(Z_q + w_{(i,j)}, 2) = 1 \\ (Z_q + 1/2) * q, & \text{if } \text{mod}(Z_q + w_{(i,j)}, 2) = 0 \end{cases} \quad (9)$$

where  $w_{(i,j)} \in W_{nRONI}$ ,  $i = 1, 2 \dots 64$ ,  $j = 1, 2 \dots 64$ ,  $I'_{dct}$  is the middle-frequency vector after watermark embedding.

7)  $I'_{dct}$  will replace the middle-frequency coefficients from 13 to 19 in the zigzag sequence. Then, an inverse zigzag is used to obtain the original DCT coefficients, and the one-dimensional sequence is changed into a two-dimensional matrix.

8) The inverse DCT transform is used to reconstruct and create the watermarked RONI. The watermark embedding procedure is represented in Figure 3.

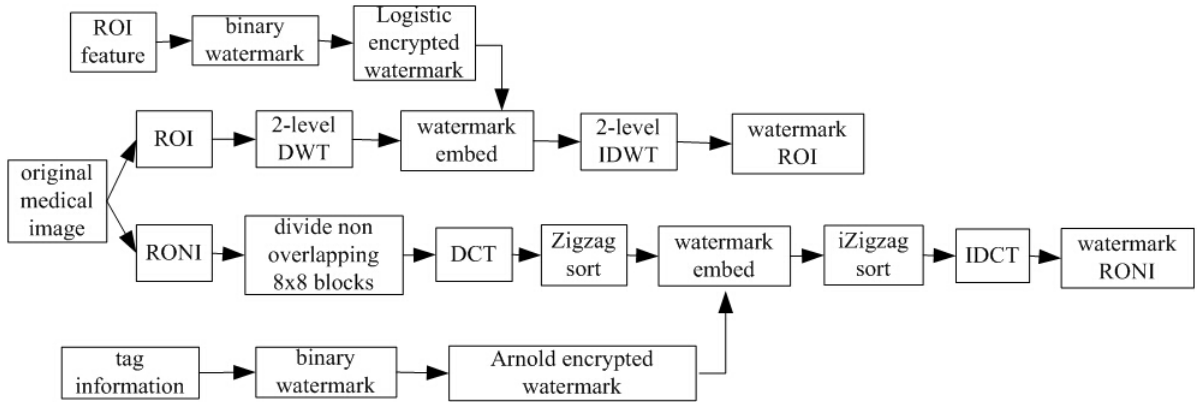


FIGURE 3. Embedding process

### 3.5. Extraction Scheme.

#### Step 1. Watermark extraction for ROI.

1) The detected medical image is divided into the ROI and RONI using the transmitted key. The watermarked ROI is decomposed into two-levels using DWT. Then, we get the low-frequency component.

2) The calculation formula for the quantization step is shown as follow.

$$Z'_Q = \text{round}(LL'_2/Q') \quad (10)$$

where  $Q'$  is obtained by using the same formula (3).

3) Supposing  $W'_{sROI}$  is the extracted watermark, the formula is shown as follow.

$$W'_{sROI} = \text{mod}(Z'_Q, 2) \quad (11)$$

4) Because the extracted watermarking image is encrypted, the original watermarking image  $W'_{ROI}$  is obtained by applying an *XOR* operation to extract watermarking image  $W'_{sROI}$  and two-dimensional matrix  $S$ .

$$W'_{ROI} = W'_{sROI} \oplus S \quad (12)$$

5) Apply the *XOR* operation to the original watermarking image  $W'_{ROI}$  and original watermarking image  $W_{ROI}$  to get the tampered watermarking image. From the tampered watermarking image, we can locate the tampered position. If the image is not modified, little noises will be included in the tampered image. If the general image content has been modified and is tampered in a small area, the noises will be focused.

### Step 2. Watermark extraction for RONI.

- 1) The watermarked RONI is divided into non-overlapping  $8 \times 8$  blocks, and the DCT transform is applied to each block.
- 2) The coefficients of each block are sorted using the zigzag sequence, and we get a one-dimensional row vector. The middle-frequency coefficients from 13 to 19 are selected.
- 3) The coefficients are quantized using the following quantization formula.

$$Z'_q = \text{floor}(I''_{dct}/q) \quad (13)$$

where  $I''_{dct}$  is the coefficients of each block.

- 4) The watermark extraction formula is as follow.

$$W'_{nRONI} = \text{mod}(Z'_q, 2) \quad (14)$$

using cycle of Arnold for  $W'_{nRONI}$ , we get the original watermark  $W'_{RONI}$ , and obtain the tag information of the medical image. Figure 4 shows the whole extracting process.

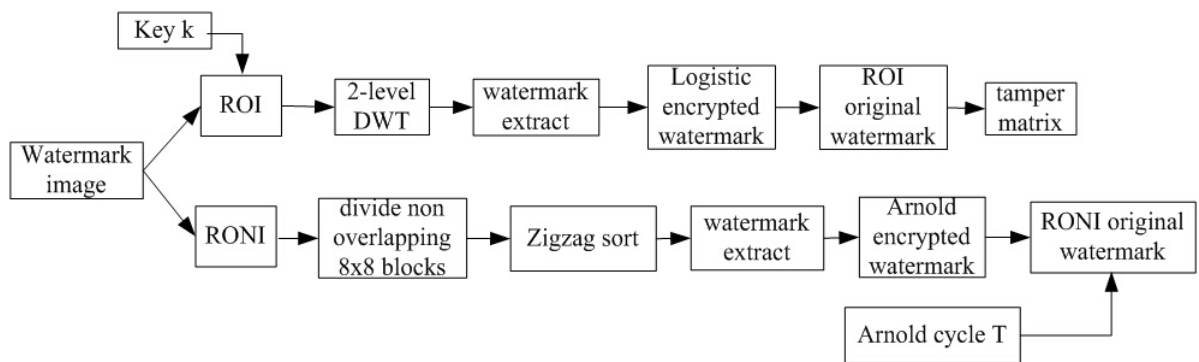


FIGURE 4. Extracting process

**4. Testing of Various Attacks.** In this section, some experimental results of using the algorithm for medical images are given. We have implemented the algorithm under the Matlab 7.0 environment. The size of the original medical image was  $512 \times 512$ . The original medical image was divided into the ROI and RONI, as shown in Figure 5.

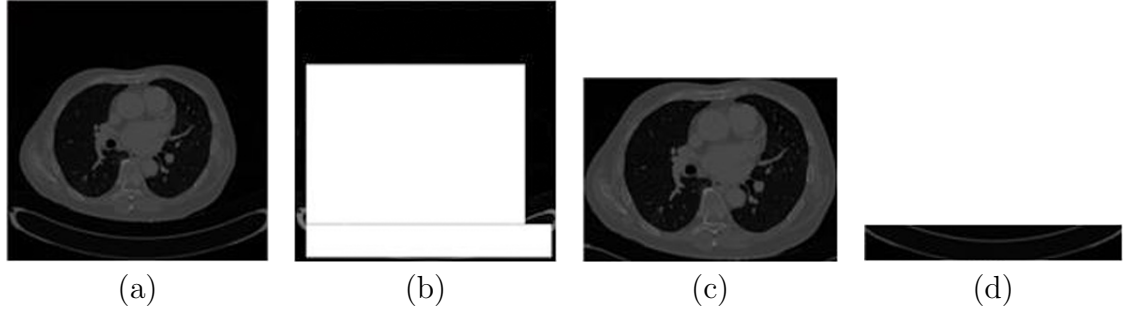


FIGURE 5. (a) Original medical image; (b) Image after cropping ROI and RONI; (c) ROI; (d) RONI

**4.1. Testing the embedded watermark of ROI with common attacks.** In this section, we will test the watermark embedded into ROI with common attacks. Results will be given in Figure 6.

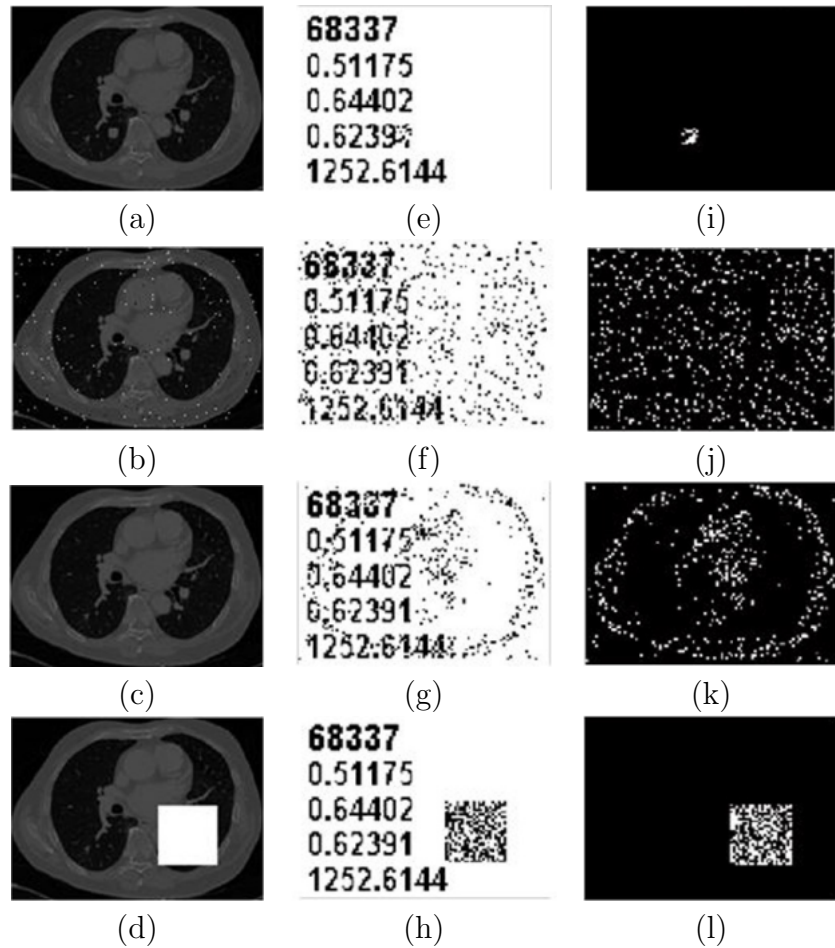


FIGURE 6. (a) Copy a part to another region in ROI; (b) Add the salt and pepper noise with density of 0.01 to ROI; (c) Add the gauss noise to ROI; (d) Crop a part from ROI; (e) Watermark extracted from (a); (f) Watermark extracted from (b); (g) Watermark extracted from (c); (h) Watermark extracted from (d); (i)(j)(k)(l) Show binary error maps

More medical images will be tested with copy, crop attacks. Results will be given in Figure 7.

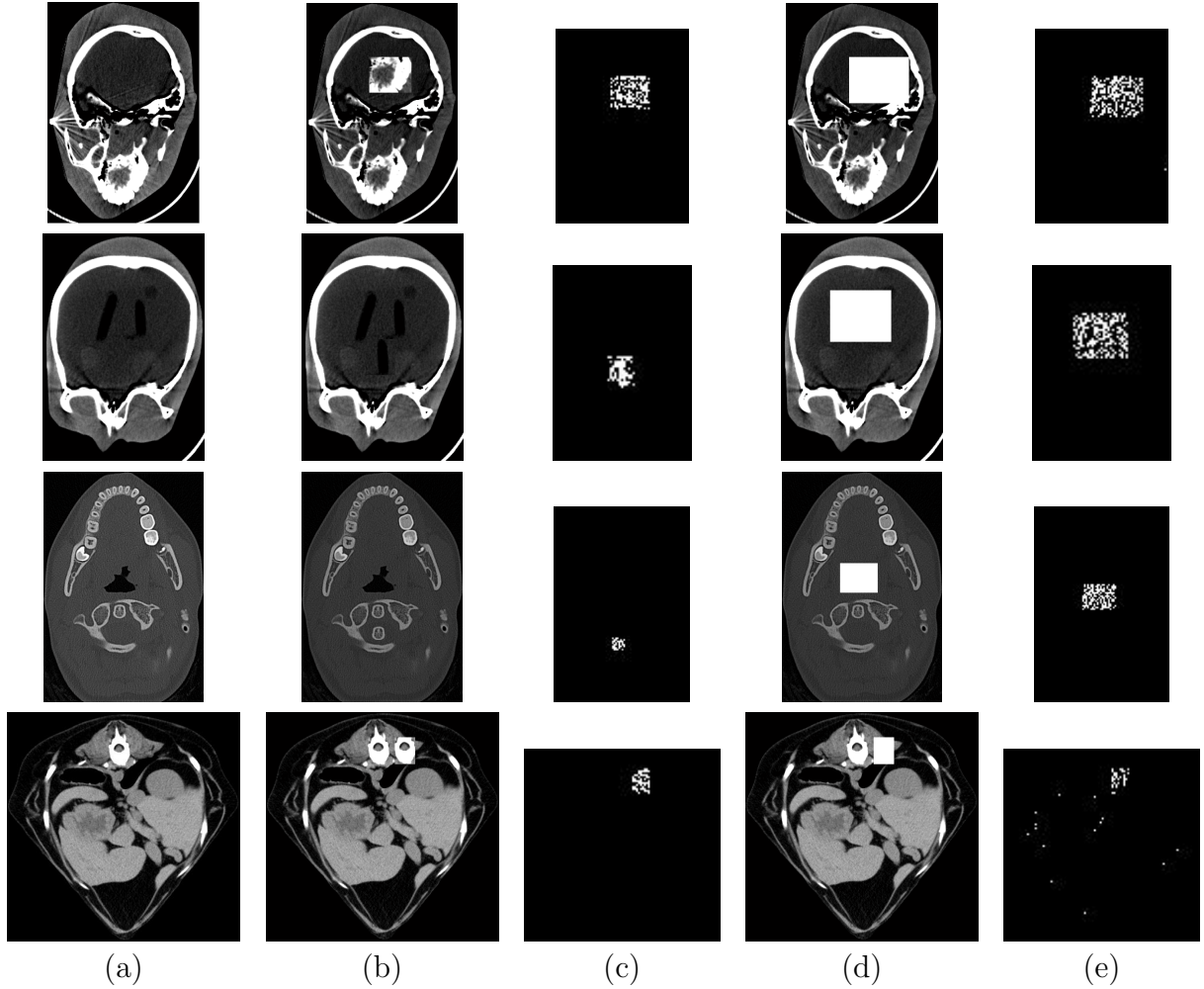


FIGURE 7. (a) Watermarked image; (b) Copy a part to another region in ROI; (c) Show binary error maps; (d) Crop a part from ROI; (e) Show binary error maps

Medical images will be tested with noise attacks. Results will be given in Figure 8.

**4.2. Testing the embedded watermark of RONI with common attack.** In this section, we will test the watermark embedded into RONI with common attacks. Results will be given in Figure 9 and the normalized coefficient (NC) will be shown in Table 2.

TABLE 2. The normalized coefficient (NC) of watermark

Title	(a)	(b)	(c)	(d)
NC	0.9900	0.9698	0.9822	0.9974

From these figures and tables, the content of the watermarked image extracted from RONI can still be seen clearly.

**5. Experimental Results and Discussions.** To evaluate this scheme, various image quality measures are used such as PSNR, SSIM, and NC.

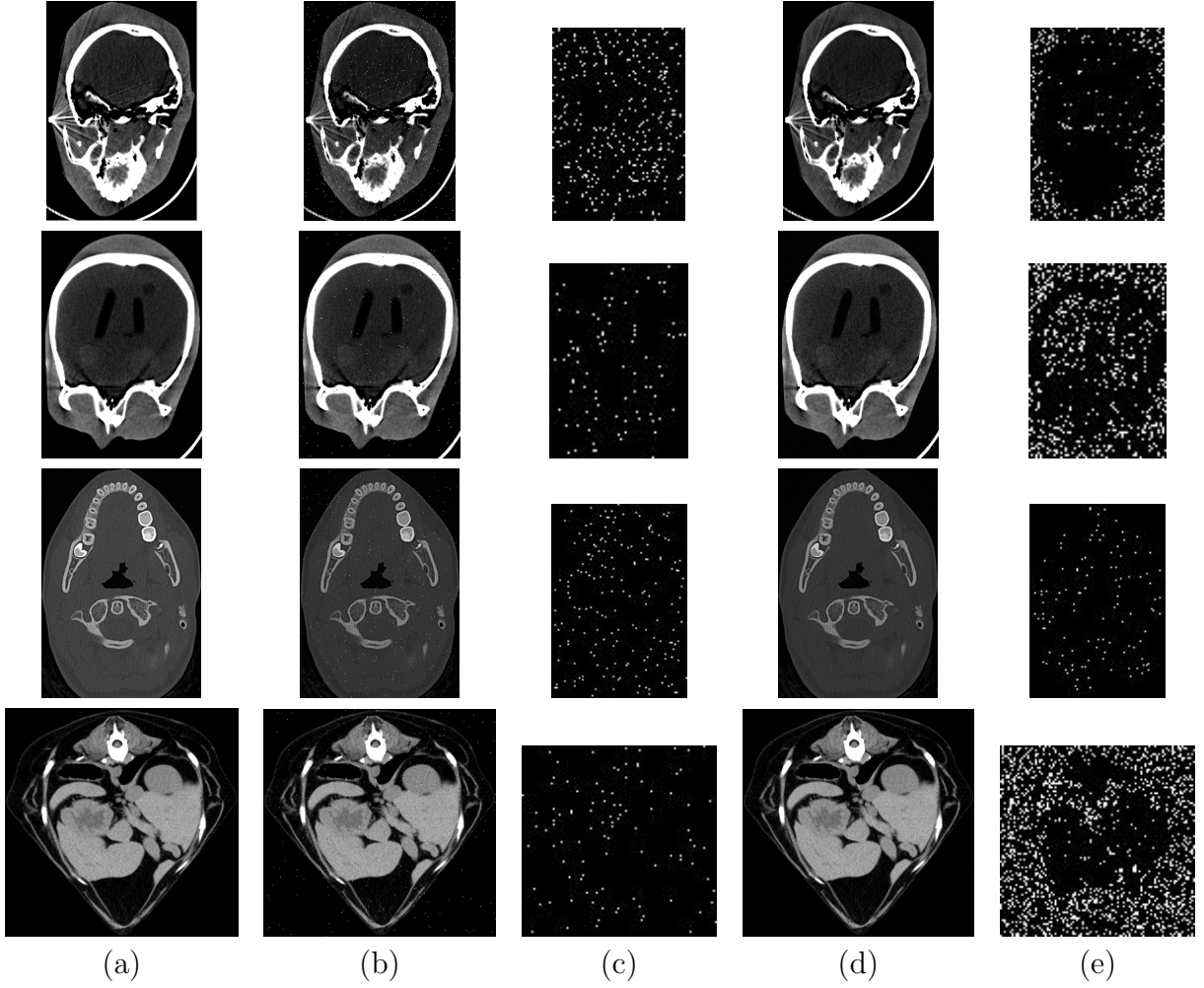


FIGURE 8. (a) Watermarked image; (b) Add the salt and pepper noise to ROI; (c) Show binary error maps; (d) Add the gauss noise to ROI; (e) Show binary error maps

**5.1. Peak Signal to Noise Ratio (PSNR).** PSNR [10] is always used to measure the objective image quality. The formula is shown as follows.

$$PSNR = 10 \log_{10} \left( \frac{(B - 1)^2}{MSE} \right) \quad (15)$$

where  $B$  is the binary digit of an image pixel.  $MSE$  is the mean square error between the original image and the embedded watermark image. The value of  $PSNR$  is greater, because it has less distortion.  $MSE$  [10] is

$$MSE = \frac{\sum_{i=1}^m \sum_{j=1}^n (I_{ij} - I'_{ij})^2}{m \times n} \quad (16)$$

**5.2. Structural Similarity Index Measurement (SSIM).** SSIM system is another measurement method used in this paper. In recent years, it has been widely used to measure image quality because it overcomes some of the inherent limitations of PSNR. The system estimates the structure change between two complex signal structures. This metric is ideal for testing the similarities of medical images because it focuses on local rather than global image similarity [10].

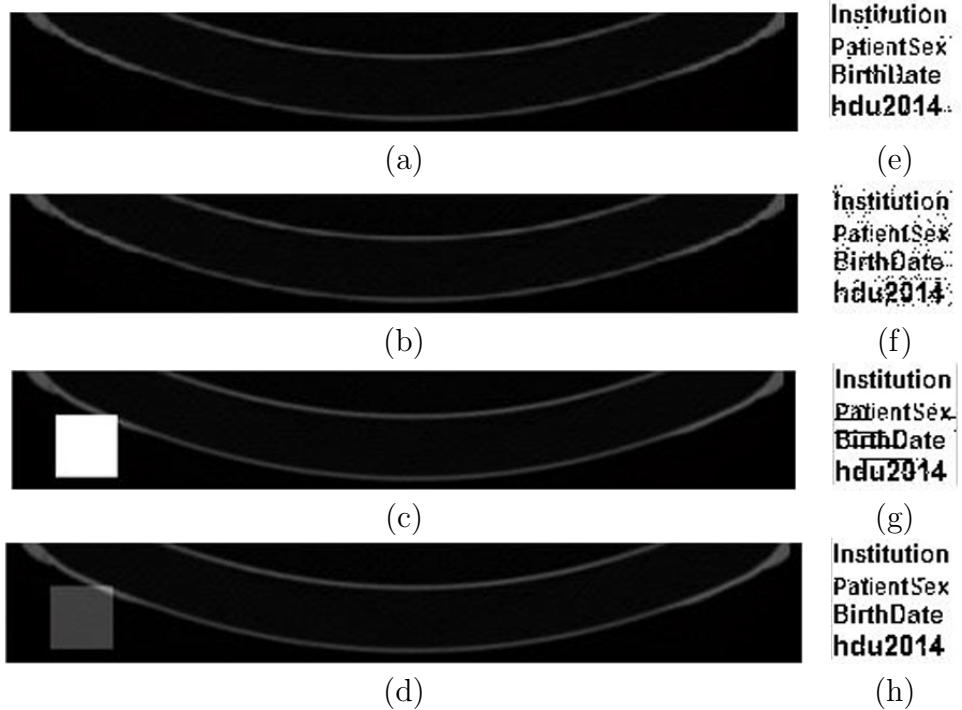


FIGURE 9. (a) Add the salt and pepper noise with density of 0.001 to RONI; (b) Add the Gauss noise to RONI; (c) Crop a part from RONI; (d) Add the value of gray for a part of RONI; (e) Watermark extracted from (a); (f) Watermark extracted from (b); (g) Watermark extracted from (c);(h) Watermark extracted from (d)

**5.3. Normalized Coefficient (NC).** NC gives a measure of the quantitative similarity between the extracted and embedded watermarking. The formula is shown as follows.

$$NC = \frac{\sum_{i=1}^m \sum_{j=1}^n W_{ij} W'_{ij}}{\sum_{i=1}^m \sum_{j=1}^n W_{ij}^2} \quad (17)$$

The comparative results of the two schemes for same medical images with different steps are listed in Table 3.

Therefore, this algorithm is better than the method in the literature [22].

**5.4. False Alarm Rate.** False alarm rate is the number of noises in the binary watermark error map. Results of the false alarm test will be seen in Figure 10.

Compared with the literature [22], the false alarm rate is low in our scheme without any attacks. Therefore, this algorithm is better than the method in the literature [22].

**6. Conclusions.** In this paper, a multiple watermarking scheme has been proposed based on DWT-DCT quantization for medical images. The medical image is divided into the region of interest (ROI) and region of non-interest (RONI). The feature information of the connected region in the ROI and tag information are contained in the original medical image as watermark. The 2-level DWT is applied to the ROI and the low frequency coefficients are quantized to embed the watermark into the ROI. It is robust to common attacks, and can be used to detect the tampered region. After dividing the RONI into  $8 \times 8$  non overlapping blocks, DCT is used to each block and the DCT coefficients of each block are sorted by zigzag transform. The intermediate frequency coefficients are quantized to

TABLE 3. The comparison of the two schemes with different quantized steps

Our scheme	PSNR	SSIM	Literature[22]	PSNR	SSIM
<b>Im1</b>			<b>Im1</b>		
<b>K = 8</b>	58.2538	0.9988	<b>q = 48</b>	53.7433	0.9918
<b>K = 16</b>	52.2416	0.9949	<b>q = 96</b>	47.7682	0.9698
<b>K = 32</b>	46.2002	0.9807	<b>q = 192</b>	42.0048	0.9047
<b>K = 64</b>	40.4967	0.9261	<b>q = 384</b>	35.4025	0.7392
<b>Im2</b>			<b>Im2</b>		
<b>K = 8</b>	58.9357	0.9989	<b>q = 48</b>	53.6950	0.9919
<b>K = 16</b>	52.9217	0.9955	<b>q = 96</b>	47.7995	0.9705
<b>K = 32</b>	47.0634	0.9833	<b>q = 192</b>	42.0756	0.9066
<b>K = 64</b>	41.1363	0.9267	<b>q = 384</b>	35.4749	0.7397
<b>Im3</b>			<b>Im3</b>		
<b>K = 8</b>	55.4412	0.9988	<b>q = 48</b>	54.0437	0.9986
<b>K = 16</b>	49.5646	0.9953	<b>q = 96</b>	48.0809	0.9951
<b>K = 32</b>	43.4759	0.9810	<b>q = 192</b>	42.0203	0.9807
<b>K = 64</b>	36.8578	0.9205	<b>q = 384</b>	36.3126	0.9201
<b>Im4</b>			<b>Im4</b>		
<b>K = 8</b>	55.7670	0.9986	<b>q = 48</b>	55.5645	0.9979
<b>K = 16</b>	49.8199	0.9944	<b>q = 96</b>	49.5357	0.9917
<b>K = 32</b>	43.7678	0.9768	<b>q = 192</b>	42.8856	0.9631
<b>K = 64</b>	37.9873	0.9266	<b>q = 384</b>	37.3889	0.8952
<b>Im5</b>			<b>Im5</b>		
<b>K = 8</b>	63.6916	0.9993	<b>q = 48</b>	52.2505	0.9818
<b>K = 16</b>	57.7763	0.9971	<b>q = 96</b>	46.2766	0.9332
<b>K = 32</b>	52.2737	0.9900	<b>q = 192</b>	40.1840	0.7934
<b>K = 64</b>	46.0951	0.9594	<b>q = 384</b>	33.9186	0.5349

embed the watermark into the RONI. The algorithm can enhance the robustness of the watermark and enhance the ability to resist common attacks. It is practical for medical image application to implement the tracking of the user that download medical images on the network and the tampering localization of the image.

**Acknowledgements.** This work was partially supported by the National Key Technology Research and Development Program of the Ministry of Science and Technology of China (No. 2012BAH91F03) and National Natural Science Foundation of China (No.61370218).

## REFERENCES

- [1] Adiwijaya, P. N. Faoziyah, F. P. Permana, T. A. B. Wirayuda, and U. N. Wisesty, Tamper detection and recovery of medical image watermarking using modified LSB and huffman compression, *Proc. of 2013 Second International Conference on Informatics & Applications (ICIA)*, pp. 129-132, 2013.
- [2] J.Cai, P. Ye, and T. Liu, A semi-fragile watermarking algorithm for medical image based on wavelet transform, *Computer Applications and Software*, vol. 27, no. 2, pp. 78-84, 2007.
- [3] G. Coatrieux, H. Huang, H. Shu, L. Luo and C. Roux, A watermarking-based medical image integrity control system and an image moment signature for tampering characterization, *IEEE Journal of Biomedical and Health Informatics*, vol. 17, no. 6, pp. 1057-1067, 2013.
- [4] S. Das and M.K. Kundu, Effective management of medical information through ROI-lossless fragile image watermarking technique, *Computer Methods and Programs in Biomedicine*, vol. 111, no. 3, pp.662-675, 2013.

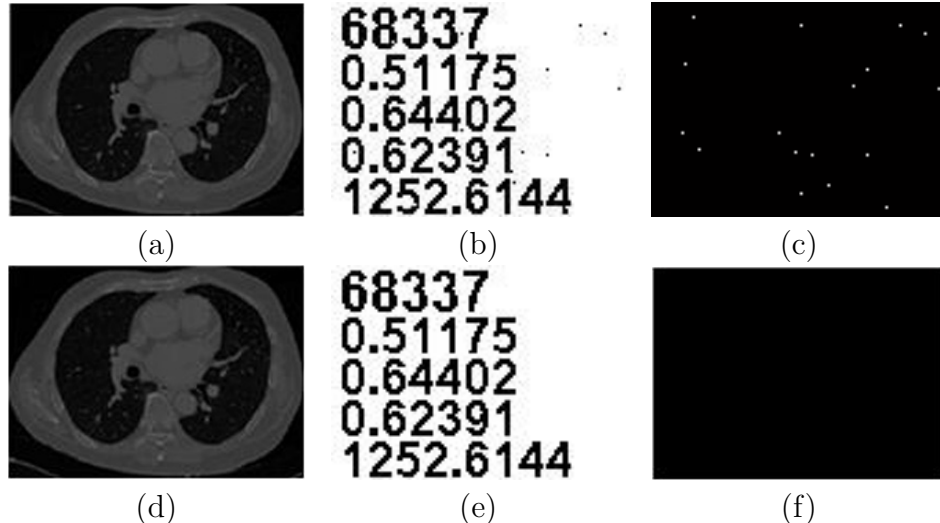


FIGURE 10. (a) Watermarked ROI with Literature[22]; (b) Binary watermark extracted from (a); (c) Binary watermark error map of (a); (d) Watermarked ROI with our scheme; (e) Binary watermark extracted from (d); (f) Binary watermark error map of (d)

- [5] C. Dong, J. Li, M. Huang and Y. Bai, The medical image watermarking algorithm with encryption by dct and logistic, *Proc. of Web Information Systems and Applications Conference (WISA)*, pp. 119-124, 2012.
- [6] F.E.-Z. A. Elgamal, N.A. Hikal, and F. E. Z. Abou-Chadi, A trust management scheme for sharing secure medical images over cloud computing environment, *Journal of Advances in Computer Network*, vol .1, no. 3, pp.201-207, 2013.
- [7] Q. Feng, L. Chen and F. Yang, A fragile watermarking scheme for medical images based on integral wavelet transform, *Journal of Image and Graphics*, vol. 11, no. 5, pp. 736-741, 2006.
- [8] W. Fu and G. Xing, Research on blind watermarking embedding algorithm with replacing middle frequency coefficients in DCT domain, *Application Research of Computers*, vol. 24, no. 3, pp. 160-162, 2007.
- [9] A. Giakoumaki, S. Pavlopoulos and D. Koutsouris, Secure and efficient health data management through multiple watermarking on medical images, *Medical & Biological Engineering & Computing*, vol. 44, no.8, pp. 619-631, 2006.
- [10] Q. Gu and T. Gao, A novel reversible watermarking scheme based on block energy difference for medical images, *Proc. of 2012 Joint 6th International Conference on Soft Computing and Intelligent Systems (SCIS 2012) and 13th International Symposium on Advanced Intelligent Systems (ISIS 2012)*, vol. 26, no. 3, pp. 355-361, 2006.
- [11] S.I. Hisham, A.N. Muhammad, J.M. Zain, G. Badshah and N.W. Arshad, Digital Watermarking for recovering attack areas of medical images using spiral numbering, *Proc. of 2013 International Conference on Electronics, Computer and Computation (ICECCO)*, pp. 285-288, 2013.
- [12] A. Kannammal and S.S. Rani, Two level security for medical images using watermarking/encryption algorithms, *International Journal of Imaging Systems and Technology*, vol. 24, pp. 111-120, 2014.
- [13] E.P. Kumar, R.E. Philip, P.S. Kumar and M.G. Sumithra, DWT-SVD based reversible watermarking algorithm for embedding the secret data in medical images, *Proc. of 2013 Fourth International Conference on Computing, Communications and Networking Technologies (ICCCNT)*, pp.1-7, 2013.
- [14] X. Li, Optimization analysis of formulas for quantization-based image watermarking, *Opto-Electronic Engineering*, vol. 37, no. 2, pp. 96-102, 2010.
- [15] J. Li, Y. Liu, W. Du, Yen-wei Chen, The robust medical image watermarking using logistic map, *Journal of Convergence Information Technology*, vol. 8, no. 5, pp. 884-892, 2013.
- [16] J. Li, Y. Liu, X. Han and Y. Chen, DFT based multiple robust watermarks for medical image, *Journal of Convergence Information Technology*, vol. 8, no. 4, pp. 860-868, 2013.

- [17] L. Lv, H. Fan, J. Wang and Y. Yang, A semi-fragile watermarking scheme for image tamper localization and recovery, *Journal of Theoretical and Applied Information Technology*, vol. 42, no. 2, pp. 287-291, 2012.
- [18] M.T. Naseem, I.M. Qureshi, Atta-ur-Rahman and M.Z. Muzaffar, Chaos based invertible authentication of medical images, *Proc. of 2013 IEEE 9th International Conference on Emerging Technologies (ICET)* , pp. 1-5, 2013.
- [19] H. Nyeem, W. Boles and C. Boyd, A review of medical image watermarking requirements for telera-diology, *Journal of Digital Imaging*, vol. 26, no. 2, pp. 326-343, 2013.
- [20] H. Nyeem, W. Boles and C. Boyd, Utilizing least significant bit-planes of roni pixels for medical image watermarking, *Proc. of 2013 International Conference on Digital Image Computing: Techniques and Applications (DICTA)*, pp. 1-8, 2013.
- [21] R.O. Preda, Semi-fragile watermarking for image authentication with sensitive tamper localization in the wavelet domain, *Measurement*, vol. 46, no. 1, pp. 367-373, 2013.
- [22] X. Qi and X. Xin, A quantization-based semi-fragile watermarking scheme for image content authentication, *Journal of Visual Communication and Image Representation*, vol. 22, no. 2, pp. 187-200, 2011.
- [23] Y. Shang and Y. Kang, Medical images watermarking algorithm based on improved dct, *Journal of Multimedia*, vol. 8, no. 6, pp. 796-801, 2013.
- [24] M. Sui, J. Li, C. Dong and Y. Bai, The encrypted watermarking for medical image based on arnold scrambling and DWT, *Journal of Convergence Information Technology*, vol. 8, no. 5, pp.893-902, 2013.
- [25] X. Wang and L. Chen, A novel adaptive semi-fragile watermarking scheme based on image content, *Acta Automatica Sinica*, vol. 33, no. 4, pp. 361-366, 2007.
- [26] Y. Wang, H. Lin and S. Yang, A large capacity watermark algorithm based on DCT transform, *Proc. of Research and Application of Image and Graphics Technologies*, pp.220-224, 2010.
- [27] L. Wu, J. Zhang, W. Deng and D. He, Arnold transformation algorithm and anti-arnold transformation algorithm, *Proc. of Information Science and Engineering (ICISE)*, pp.1164-1167, 2009.
- [28] J. Ying, Q. Liu and C. Liu, An adaptive semi-fragile watermarking algorithm based on wavelet low frequency coefficients, *Proc. of International Conference on Communications, Electronics and Automation Engineering*, pp. 1011-1018, 2013.
- [29] X. Zhang, L. Cui, and L. Shao, A fast semi-fragile watermarking scheme based on quantizing the weighted mean of integer haar wavelet coefficients, *Proc. of 2012 Symposium on Photonics and Optoelectronics (SOPO 2012)*, pp. 1-4, 2012.
- [30] X. Zhao and Y. Kang, The semi-fragile digital watermark embedding algorithm based on second-generation wavelet, *Proc. of 2011 International Conference on Transportation and Mechanical & Electrical Engineering (TMEE)* ,pp.1721-1724, 2011.